Anal. Chem. **2006,** *78,* 5711−5718

Quantitative Determination of Absolute Organohalogen Concentrations in Environmental Samples by X-ray Absorption Spectroscopy

Alessandra C. Leri,*,† Michael B. Hay,‡ Antonio Lanzirotti,|| William Rao,§ and Satish C. B. Myneni⊥,#

Departments of Chemistry, Geosciences, and Civil and Environmental Engineering, Princeton University, Princeton, New Jersey 08544, Consortium for Advanced Radiation Sources, The University of Chicago, 5640 South Ellis Avenue, Chicago, Illinois 60637, Savannah River Ecology Laboratory, University of Georgia, Aiken, South Carolina 29802, and Earth Sciences Division, Lawrence Berkeley National Laboratory, 1 Cyclotron Road, Berkeley, California 94720

An in situ procedure for quantifying total organic and inorganic Cl concentrations in environmental samples based on X-ray absorption near-edge structure (XANES) spectroscopy has been developed. Cl 1*s* XANES spectra reflect contributions from all Cl species present in a sample, providing a definitive measure of total Cl concentration in chemically heterogeneous samples. Spectral features near the Cl K-absorption edge provide detailed information about the bonding state of Cl, whereas the absolute fluorescence intensity of the spectra is directly proportional to total Cl concentration, allowing for simultaneous determination of Cl speciation and concentration in plant, soil, and natural water samples. Absolute Cl concentrations are obtained from Cl 1*s* XANES spectra using a series of Cl standards in a matrix of uniform bulk density. With the high sensitivity of synchrotron-based X-ray absorption spectroscopy, Cl concentration can be reliably measured down to the 5−10 ppm range in solid and liquid samples. Referencing the characteristic near-edge features of Cl in various model compounds, we can distinguish between inorganic chloride (Cl_{inorg}) and organochlorine (Cl_{org}), as well as between aliphatic Cl_{org} and aromatic Cl_{org}, with uncertainties in the range of ∼6%. In addition, total organic and inorganic Br concentrations in sediment samples are quantified using a combination of Br 1*s* XANES and X-ray fluorescence (XRF) spectroscopy. Br concentration is detected down to ∼1 ppm by XRF, and Br 1*s* XANES spectra allow quantification of the Br_{inorg} and Br_{org} fractions. These procedures provide nondestructive, element-specific techniques for quantification of Cl and Br concentrations that preclude extensive sample preparation.

Halogens participate in complex biogeochemical transformations in terrestrial systems, cycling between organic and inorganic forms.[1−7] Naturally produced organohalogens include a diverse array of relatively low molecular weight molecules,[8,9] as well as macromolecules of indeterminate structure, such as humic substances.[10,11] Despite the ubiquity of natural organohalogen molecules, the processes associated with their formation and degradation in the environment remain poorly understood. Investigation of halogen fluxes has been limited by the inadequacy of available techniques to account for the myriad chemical forms of halogens in heterogeneous soil, sediment, plant, and aqueous samples. In particular, quantitative methods requiring chemical isolation of organohalogen fractions from natural samples are prone to partial recoveries, chemical alterations of halogens, or both. Here, we present the applications of synchrotron-based X-ray fluorescence (XRF) and X-ray absorption near-edge structure (XANES) spectroscopy to the in situ determination of absolute Cl_{org} and Br_{org} concentrations in natural samples. Robust, quantitative information about organohalogen fluxes in soil and sediment systems will help complete the description of natural halogen cycles, possibly illuminating the sources and sinks of naturally and industrially produced organohalogens in the environment.

Organohalogens in the environment appear in aqueous, gaseous, and solid phases. Although in situ, nondestructive methods exist for measuring total halogen concentrations,[12−16]

* Corresponding author. E-mail: aleri@princeton.edu.
† Department of Chemistry, Princeton University.
‡ Department of Civil and Environmental Engineering, Princeton University.
|| Consortium for Advanced Radiation Sources, The University of Chicago.
§ Savannah River Ecology Laboratory, University of Georgia.
⊥ Department of Geosciences, Princeton University.
Earth Sciences Division, Lawrence Berkeley National Laboratory.

(1) Hjelm, O.; Johansson, E.; Öberg, G. *Soil Biol. Biochem.* **1999**, *31*, 1509−1515.
(2) Öberg, G. *Appl. Microbiol. Biotechnol.* **2002**, *58*, 565−581.
(3) Bergbauer, M.; Eggert, C.; Kraepelin, G. *Appl. Microbiol. Biotechnol* **1991**, *35*, 105−109.
(4) Joshi, D. K.; Gold, M. H. *Appl. Environ. Microbiol.* **1993**, *59*, 1779−1785.
(5) Valli, K.; Wariishi, H.; Gold, M. H. *J. Bacteriol.* **1992**, *174*, 2131−2137.
(6) Ahn, Y. B.; Rhee, S. K.; Fennell, D. E.; Kerkhof, L. J.; Hentschel, U.; Haggblom, M. M. *Appl. Environ. Microbiol.* **2003**, *69*, 4159−4166.
(7) Neidleman, S. L.; Geigert, J. *Biohalogenation: Principles, Basic Roles and Applications*; Ellis Horwood Limited: Chichester, 1986.
(8) Gribble, G. W. *Chemosphere* **2003**, *52*, 289−297.
(9) Gribble, G. W. *Chem. Soc. Rev.* **1999**, *28*, 335−346.
(10) Muller, G.; Nkusi, G.; Scholer, H. F. *J. Prakt. Chem.* **1996**, *338*, 23−29.
(11) Myneni, S. C. B. *Science* **2002**, *295*, 1039−1041.
(12) Heinrich, C. A.; Bain, J. H. C.; Fardy, J. J.; Waring, C. L. *Geochim. Cosmochim. Acta* **1993**, *57*, 2991−3000.
(13) Alamin, M. B.; Spyrou, N. M. *J. Radioanal. Nucl. Chem.* **1997**, *216*, 41−45.
(14) Necemer, M.; Kump, P.; Rajcevic, M.; Jacimovic, R.; Budic, B.; Ponikvar, M. *Spectrochim. Acta, Part B* **2003**, *58*, 1367−1373.
(15) Yamada, Y. *Talanta* **1968**, *15*, 1135−1141.
(16) Ristori, G. G.; Fusi, P.; Bruno, V. *Agrochimica* **1971**, *15*, 427−433.

10.1021/ac060476m CCC: $33.50
Published on Web 07/20/2006

in situ techniques for quantifying absolute organohalogen concentrations in chemically heterogeneous samples are not available. Established quantitative assays for nonvolatile halogen species in natural samples target (1) total halogen concentrations by element (e.g., XRF, instrumental neutron activation analysis [INAA]), (2) total organohalogen concentrations (e.g., the adsorbable organohalogen [AOX] sum parameter), (3) total inorganic halide concentrations (e.g., $AgNO_3$-based titrimetry, ion chromatography), or (4) the concentrations of one or several specific organohalogen molecules (e.g., gas chromatography/mass spectrometry). Although INAA and XRF are capable of measuring total halogen concentrations in solid phase samples, neither yields information on the chemical forms of the halogens present. Aside from INAA and XRF, the aforementioned methods require that the environmental sample be aqueous phase or a liquid extract of a solid phase sample. This means that no existing analytical technique provides a direct measurement of total organohalogen concentrations in unextracted soil, plant, and sediment samples. The established methods to measure organohalogen concentrations in solid-phase extracts may be efficient for relatively low molecular weight organohalogens but may not detect all organohalogen molecules in complex mixtures, many of which are likely to be unextractable macromolecules in the case of environmental samples.

At present, total organohalogen concentrations in soils, sediments, and natural waters are typically reported on the basis of the AOX sum parameter (EU standard procedure 1485, 1996). The AOX procedure involves reaction of acidified aqueous samples or solid-phase extracts with activated carbon prior to combustion and detection of hydrogen halides by microcoulometric titration with Ag^+ ions.[1,17−19] This technique features low detection limits (∼5 ppm)[19] but fails to distinguish among the halogens and is subject to interference from inorganic halides.[20,21] In addition, AOX, like any technique that relies on chemical processing, poses a risk of chemical transformations (low pH conditions in particular favor the oxidation of halide ions), incomplete recoveries, or both.

Our goal, therefore, was to measure total Cl_{org} and Br_{org} concentrations in environmental samples, particularly soils and sediments, without performing chemical isolation procedures. We achieved this using a combination of synchrotron-based XRF analysis and XANES spectroscopy.

Organohalogen Analysis via XRF and XANES Spectroscopy. Synchrotron-based XRF analysis provides in situ measurements of total elemental concentrations with detection limits reaching trace levels (∼1 ppm). In XRF spectroscopy, the X-ray emission associated with core-level electronic excitations in a sample is used to identify the element of interest and its concentration. The X-ray emission energy is characteristic of the element, while the intensity is proportional to the elemental concentration. The element specificity of core-level electronic transitions screens out interferences from components apart from the element of interest, making this technique well-suited to the analysis of chemically complex environmental samples. However, Si and Ge solid-state detectors, with energy resolutions in the range of 120−140 eV, are not sensitive enough to resolve the emission peaks of low-Z halogens (F, Cl) from those of neighboring elements in the periodic table (such as S in the case of Cl). This is not an issue for high-Z halogens (Br, I), the emission peaks of which are separated by several hundred eV from those of their nearest neighbors.

All natural samples contain high levels of S, to the extent that the S Kβ peak at 2464 eV overwhelms the Cl Kα peak at 2622 eV, making the emission lines of Cl and S inseparable. To avoid interference from S, we base Cl concentration measurements on Cl 1*s* XANES spectra. At energies close to the Cl K-absorption edge, the spectral features arising from the excitations of Cl 1*s* electrons exhibit a distinct structure, depending on the bonding state of Cl, allowing different forms of Cl_{inorg} and Cl_{org} to be distinguished.[11] Beyond the near-edge oscillations, fluorescence intensity levels out, becoming independent of Cl speciation and directly proportional to Cl concentration. Thus, the absolute Cl fluorescence intensity determined at an energy value well above the Cl K-absorption edge provides the basis for our total Cl concentration measurements.

In contrast to Cl, the Br Kα emission peak is well-resolved from other emission lines. Here, we measure Br concentrations in estuarine and marine sediment samples on the basis of Br Kα emission peaks, following established techniques.[15,16] The novelty of our application lies in the combination of quantitative information from XRF with Br speciation information from Br 1*s* XANES spectra to determine the absolute concentrations of Br_{org} and Br_{inorg} in the samples. Br concentrations could also be measured on the basis of Br 1*s* XANES spectra in a manner analogous to the procedure described above for Cl. However, concentration estimates based on XANES spectral analysis require significantly longer data acquisition times (∼20−30×) and offer poorer detection limits (∼10×) than XRF.

This method was developed to provide in situ measurements of absolute organohalogen concentrations in environmental samples. Exploiting the qualitative and quantitative potential of Cl 1*s* XANES spectroscopy yields concentration measurements of different forms of Cl in chemically heterogeneous soil samples. Adding speciation information from Br 1*s* XANES spectroscopy to total Br concentration determined by traditional XRF gives in situ measurements of organic and inorganic forms of Br in chemically heterogeneous sediment samples.

EXPERIMENTAL SECTION

Preparation of Standards and Samples for Cl Measurements. All standards and select environmental samples were mixed in a matrix of poly(acrylic acid, sodium salt) (PAA) and compressed into pellets to obtain uniform bulk density. PAA (Sigma-Aldrich) was oven-dried and stored in a dehumidifier prior to sample preparation. All samples prepared using PAA were stored similarly. NaCl standard pellets of different Cl concentrations were prepared by dissolving ∼310 mg of PAA in various amounts of 1.0 mM NaCl (aq) in scintillation vials. If necessary, deionized water was added to bring the total volume of liquid to ∼5 mL before thorough mixing. Samples were dried in vacuo at room temperature in a Precision brand vacuum oven. Dried samples were finely ground using a mortar and pestle before compression into pellets. Pellets were made using a 13-mm die

(17) Öberg, G.; Brunberg, H.; Hjelm, O. *Soil Biol. Biochem.* **1997**, *29*, 191−197.
(18) Jokela, J.; Salkinoja-Salonen, M. S.; Elomaa, E. *J. Water SRT − Aqua* **1992**, *41*, 4−12.
(19) Öberg, G.; Sandén, P. *Hydrol. Processes* **2005**, *19*, 2123-2136.
(20) Berger, D. L. *Anal. Chem.* **1984**, *56*, 2271−2272.
(21) Harper, F. *Ground Water Monit. Rem.* **1984**, *4*, 46−48.

with tungsten carbide anvils under 10 tons of pressure in a standard hydraulic laboratory press. An analogous procedure was applied to the preparation of samples with varying quantities of NaCl and the soluble Cl_{org} standards, 3-chloropropionic acid (to represent aliphatic Cl_{org}), and chlorophenol red (to represent aromatic Cl_{org}).

Mulch material was air-dried for a week before being finely milled using a coffee grinder and roller mill in tandem. The resulting powder was pressed into pellets in pure form (using ~260 mg to account for the lower density of the material compared with PAA) or mixed with PAA in ratios ranging from 10 to 90% PAA by weight. The majority of the mulch analyzed consisted of senescent or decaying white oak (*Quercus alba*) leaves collected from the Brendan Byrne State Forest in the Pine Barrens of New Jersey.

Aqueous samples containing leaf leachate were obtained from our field experimental station on the Princeton University campus (NJ). At this field site, white oak leaves are allowed to weather in plastic trays suspended 5′ above ground level with leaf leachate routed into carboys below. Approximately 10 mL of aqueous leaf leachate was mixed with ~310 mg of PAA and converted into pellets according to the procedure outlined above for NaCl standards.

Cl 1s XANES Spectroscopy and Analysis. Cl 1*s* XANES spectra were acquired at beamline X19A at the National Synchrotron Light Source (NSLS), Brookhaven National Laboratory, Upton, NY. The beamline has a bending magnet source and is equipped with a fixed-exit double-crystal Si (111) monochromator. The beam is collimated and focused with a pair of Rh-coated mirrors and steered through a 10-μm thin Be window. Upstream of the sample chamber, the beam passes through an ion chamber, I_0, where the intensity of the incident beam is monitored to allow normalization of X-ray fluorescence yield (F). Both I_0 and the sample chamber were purged with He to stabilize the beam and maximize flux at the Cl K-absorption edge. Photon flux at this beamline is $\sim 5 \times 10^{10}$ photons/s at 2500 eV. The monochromator was detuned until incident photon flux was reduced by 50% to minimize high-order harmonics. The X-ray beam spot size used was 2×1 mm^2.

Sample pellets were mounted on Kapton tape and exposed directly to the incoming X-ray beam at a 45° angle. Sample fluorescence was measured over an energy range of 2800−2880 eV using a Canberra PIPS detector attached to the sample chamber. Spectral parameters were varied according to the type of analysis. For Cl concentration measurements and crude Cl speciation analysis, low-resolution spectra were collected using a 0.25-eV step size near the absorption edge and 0.5−2.0-eV step sizes above and below the edge. For detailed Cl speciation analysis, high-resolution spectra were acquired using a 0.08-eV step size around the edge and 0.1−0.5-eV step sizes above and below the edge. Labview XDAC software associated with beamline X19A was used to collect Cl 1*s* XANES spectra. The energy of the spectrometer was calibrated to the discrete absorption maximum in the Cl 1*s* XANES spectrum of chlorophenol red defined at 2821.2 eV.

Cl 1*s* XANES data were processed using SIXPack (version 0.43),[22,23] WinXAS (version 2.0),[24] PeakFit (version 4.0),[25] and MS Excel. SIXPack was used for preliminary inspection and averaging of fluorescence scans. For concentration measurements, absolute fluorescence intensity was found by fitting one straight line through the preedge region of the spectrum from 2802.3 to 2818.1 eV and another through the postedge region from 2844.8 to 2868.8 eV in MS Excel, then taking the difference between the lines at 2850.8 eV, an energy by which the postedge oscillations are attenuated (Figure 1A). Blank PAA showed a weak Cl signal, the intensity of which was subtracted from the other absolute intensity measurements to produce standard curves with y-intercepts at 0 (Figure 1B, C).

For Cl speciation analysis, SIXPack-averaged scans were imported into WinXAS for energy calibration, background subtraction, and normalization. A smooth background was obtained by fitting a first-order polynomial to the preedge region. A second first-order polynomial fit to the postedge region normalized the edge jump to 1.0 at ~2850 eV. This normalization allows for comparative analysis of spectral features in the near-edge region, where absorption intensity is dependent on Cl speciation. WinXAS was also used for nonlinear least-squares fitting of sample spectra with data from model chemical compounds to establish the speciation of Cl. PeakFit was used for deconvolution of spectra into their component peaks.

Preparation of Standards and Samples for Br Measurements. Standards for Br concentration estimates (Br XRF analyses) were prepared by homogenizing KBr in a $NaNO_3$ matrix according to the procedure described above for PAA-based NaCl standards. Different estuarine and marine sediment samples from around the globe were air-dried and ground to a fine powder in a mortar and pestle before being mixed with $NaNO_3$ (~150 mg sediment + ~250 mg $NaNO_3$) and compressed into pellets. For Br speciation measurements, Br 1*s* XANES spectra were collected on pure sediment samples sandwiched between Kapton tape and X-ray clean polyfilm (not diluted with $NaNO_3$ or compressed into pellets).

Br 1*s* XANES and XRF Spectroscopy and Analysis. For Br concentration measurements, Br Kα emission spectra were acquired at beamline X26A (energy range: 3−40 keV) at the NSLS. Beamline X26A is capable of trace element analyses with ~1 ppm sensitivity. The beamline is equipped with a Si(111) channel-cut monochromator. The X-ray beam was focused to a 12×7 μm^2 spot size using Kirkpatrick−Baez microfocusing optics. XRF spectra were collected by exciting samples with monochromatic light at 14 keV. The fluorescence signal of Br was measured using a Canberra 9-element Ge Array detector, producing MCA spectra with Kα and Kβ emission peaks corresponding to all elements present in the energy range 3−14 keV. Interactive Data Language (IDL) software associated with beamline X26A was used to collect data. Spectra were processed using an IDL-based MCA plotter. The area under the Br Kα peak was plotted against Br concentration to produce Br standard curves.

Br 1*s* XANES spectroscopic studies were conducted at the NSLS (beamline X23A2) and at the Stanford Synchrotron Radiation Laboratory (SSRL, Stanford Linear Accelerator Center, Menlo Park, CA; beamlines 2−3 and 4−3). For the collection of Br 1*s* XANES spectra, Si(311) monochromator crystals were used at

(22) Webb, S. M. *Phys. Scr. Online* **2005**, *T115*, 1011.
(23) Newville, M. *J. Synchrotron Radiat.* **2001**, *8*, 322−324.
(24) Ressler, T. *J. Synchrotron Radiat.* **1998**, *5*, 118−122.
(25) Bergbreiter, D. E.; Srinivas, B. *J. Am. Chem. Soc.* **1992**, *114*, 7961−7962.

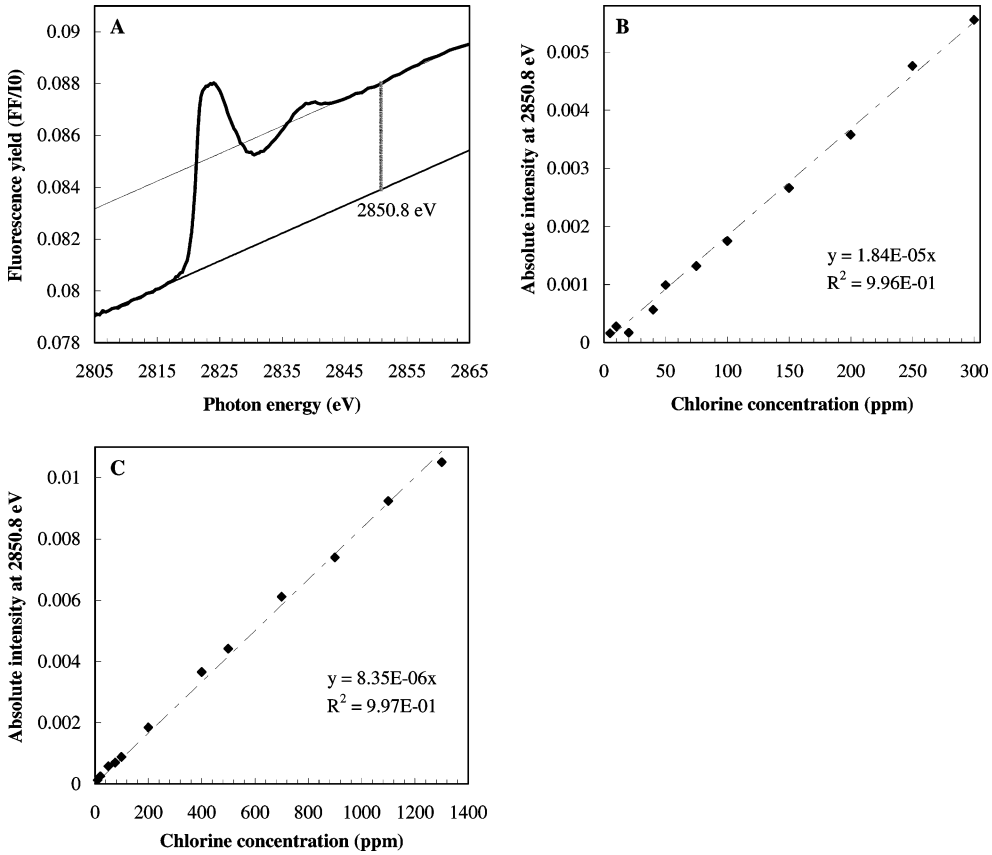

Figure 1. Quantification of Cl concentration from Cl 1*s* XANES spectra. (A) Unnormalized Cl 1*s* XANES spectrum of NaCl standard in PAA matrix (200 ppm Cl). The difference at 2850.8 eV between splines through the pre-edge and postedge regions is used as a measure of absolute Cl fluorescence intensity. (B−C) Relationship between Cl concentration in PAA-based NaCl standards and absolute Cl fluorescence intensity over different concentration ranges. The dashed lines, equations, and R^2 values represent linear fits to the data. The data in B and C were generated during different experimental beamtimes, and the difference in the *y*-scales reflects the unaccountable variations in fluorescence intensity among beamtimes. The arbitrary but systematic differences in the curves illustrate the importance of frequent standardization during measurements.

beamline X23A2, and either Si(111) or Si(220) crystals at beamlines 2−3 and 4−3. Speciation information was extracted from the Br 1*s* XANES spectra using the software and technique described above for Cl 1*s* XANES spectra. The energy of the spectrometer was calibrated according to the inflection point in the spectrum of KBr (s) at 13 474.0 eV.

RESULTS AND DISCUSSION

Quantification of Cl. Preliminary experiments suggested that the most suitable matrix material for our NaCl calibration standards would be amorphous rather than crystalline. Crystalline matrixes such as $NaNO_3$ produced diffraction peaks in the Cl 1*s* XANES region that complicated spectral analysis. An ideal matrix would also have an X-ray penetration depth similar to that of the natural organic matter (NOM) being analyzed for Cl. In addition, it was important that the matrix material be soluble in order to prepare more homogeneous NaCl standard pellets through dissolution. We found that PAA, a highly soluble polymer, provided an amorphous organic matrix that was a reasonable analogue to NOM. PAA has the advantages of hydrolytic and thermal stability, as well as low volatility, as compared with smaller chain organic molecules.

The quantitative estimation of Cl relies on the absolute fluorescence intensity of Cl 1*s* XANES spectra determined at 2850.8 eV, an energy value ~20 eV above the Cl K-absorption edge (Figure 1A). By this energy, the near-edge oscillations are attenuated, and absorption intensity is independent of Cl speciation. The PAA-based NaCl standards yield calibration curves with a strong linear relationship between Cl concentration and absolute Cl fluorescence intensity (Figure 1B, C). The correlation is linear through 1300 ppm Cl, the highest concentration measured. (The terrestrial NOM samples of interest to us typically exhibit Cl concentrations in the range of 50−500 ppm.) The linear calibration curve allows for straightforward estimation of Cl concentrations in environmental samples from their absolute Cl fluorescence intensities.

Although Cl concentration and absolute Cl fluorescence intensity are strongly correlated, the measured Cl fluorescence intensity of a sample varies significantly over long periods, particularly between synchrotron X-ray beam refills and among different experimental beamtimes (see Supporting Information). Certain sources of intensity variations can be predicted and avoided. Directly following an X-ray beam refill, for instance, it takes almost 1 h before spectra can be acquired with reproducible absolute Cl fluorescence intensity. This may be due to reequilibration of the monochromator once reinjection of the X-ray beam heats its crystals. Fluctuations in the atmospheres of the I_0 and sample chambers represent another factor that might affect

Table 1. Replicate Cl Concentration Measurements for Two Samples of White Oak Leaf Material at Different Stages of Decay

		Cl_{inorg}		aliphatic Cl_{org}		aromatic Cl_{org}	
Cl 1*s* XANES assay	total Cl (ppm)[a]	fraction[b]	concn (ppm)[c]	fraction[b]	concn (ppm)[c]	fraction[b]	concn (ppm)[c]
			Less Degraded NOM				
1	489	0.77	377	0.10	49	0.13	64
2	489	0.73	357	0.12	59	0.15	73
3	495	0.73	361	0.12	59	0.15	74
4	488	0.73	356	0.13	63	0.14	68
av	490 ± 2	0.74 ± 0.01	363 ± 5	0.12 ± 0.01	58 ± 3	0.14 ± 0.01	70 ± 2
			More Degraded NOM				
1	107	0.39	42	0.46	49	0.15	16
2	106	0.46	49	0.41	43	0.13	14
3	108	0.41	44	0.45	49	0.14	15
4	108	0.37	40	0.46	50	0.17	18
5	110	0.41	45	0.45	50	0.14	15
av	108 ± 1	0.41 ± 0.01	44 ± 2	0.45 ± 0.01	48 ± 1	0.15 ± 0.01	16 ± 1

[a] Total Cl concentrations estimated from absolute Cl fluorescence intensity in Cl 1*s* XANES spectra. Results of four to five replicate measurements on the same sample are shown, along with associated average and standard error values. Each measurement was performed at separate points between X-ray beam refills and Cl concentrations calculated on the basis of the chronologically relevant standard curve. [b] Fractions of Cl_{inorg}, aliphatic Cl_{org}, and aromatic Cl_{org} estimated via least-squares fitting of sample Cl 1*s* XANES spectra with those of model compounds of known coordination environment, for example, HCl (aq), chlorodecane, chlorophenol red. [c] Combination of Cl species fractions with total Cl concentrations gives approximate concentrations of Cl_{inorg}, aliphatic Cl_{org}, and aromatic Cl_{org} in the NOM samples (average concentrations reported with propagated error values).

reproducibility. Maintaining steady He flow rates and allowing ample purge time between samples mitigates this issue.

Even when these factors are taken into account, however, systematic variations persist. The two standard curves in Figure 1B, C were generated from the same set of NaCl standards during different experimental beamtimes. The systematic differences in the curves suggest that absolute intensity variations arise from instrumental anomalies rather than inconsistencies in the samples. These arbitrary variations illustrate the importance of frequent standardization during measurements. For this reason, relatively low-resolution Cl 1*s* XANES spectra are collected for quantitative Cl concentration measurements. Shorter data acquisition time per sample increases throughput, allowing more samples to be analyzed per standard series. The quality of the edge jump measurement is not undermined by low spectral resolution.

With frequent standardization, we obtain consistent, reproducible measurements of Cl concentration in environmental samples. Replicate total Cl concentration measurements for two samples of NOM at different stages of decay are shown in Table 1. Each measurement was performed at separate intervals between X-ray beam refills, with total Cl concentrations calculated on the basis of the chronologically relevant standard curve. The high reproducibility of Cl concentration measurements in NOM samples establishes the viability of using the absolute fluorescence intensity of Cl 1*s* XANES spectra as a measure of Cl concentration, provided that Cl standard curves are generated in parallel with measurements on natural samples.

A major obstacle to precise and accurate concentration measurements from XANES spectroscopy and similar bulk analytical techniques is matrix effects. Consistent results depend heavily on the homogeneity and uniformity of samples. To obtain samples of uniform density and thickness, all solids are pulverized, and specific quantities of the resulting powder are pressed into pellets. Relatively large X-ray beam sizes trained on the sample help minimize matrix effect errors as well. Data should ideally be collected for numerous replicate samples to ensure more statistically valid results, but this proves difficult with any synchrotron-based technique because experimental time is so limited.

Environmental samples are, in principle, heterogeneous, so particular effort must be expended to achieve thorough homogenization. Homogeneous pellets are prepared from aqueous samples in a straightforward fashion by dissolving PAA in the sample solution before drying, pulverization, and pressing. In this manner, Cl standards selected for their solubility and stability (NaCl, 3-chloropropionic acid, chlorophenol red) and aqueous leachate samples were homogenized in a PAA matrix. Aqueous sample pellets yield highly reproducible Cl concentration measurements.

Finely ground solid samples of NOM, however, have limited miscibility with PAA. After thorough mechanical mixing, pellets made out of pulverized NOM and PAA retain a mosaic appearance, and inconsistent Cl concentration measurements are testament to their chemical heterogeneity. Preparing samples from pure NOM rather than NOM mixed in a PAA matrix would reduce

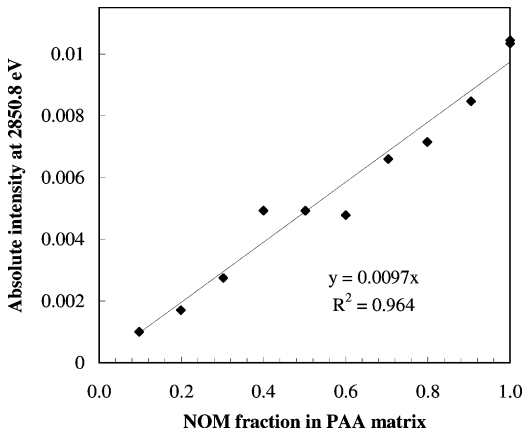

Figure 2. Absolute Cl fluorescence intensity as a function of the fraction of pulverized NOM in a PAA matrix. The linear trend suggests that differences in X-ray absorption and scattering between the PAA and NOM matrixes are negligible.

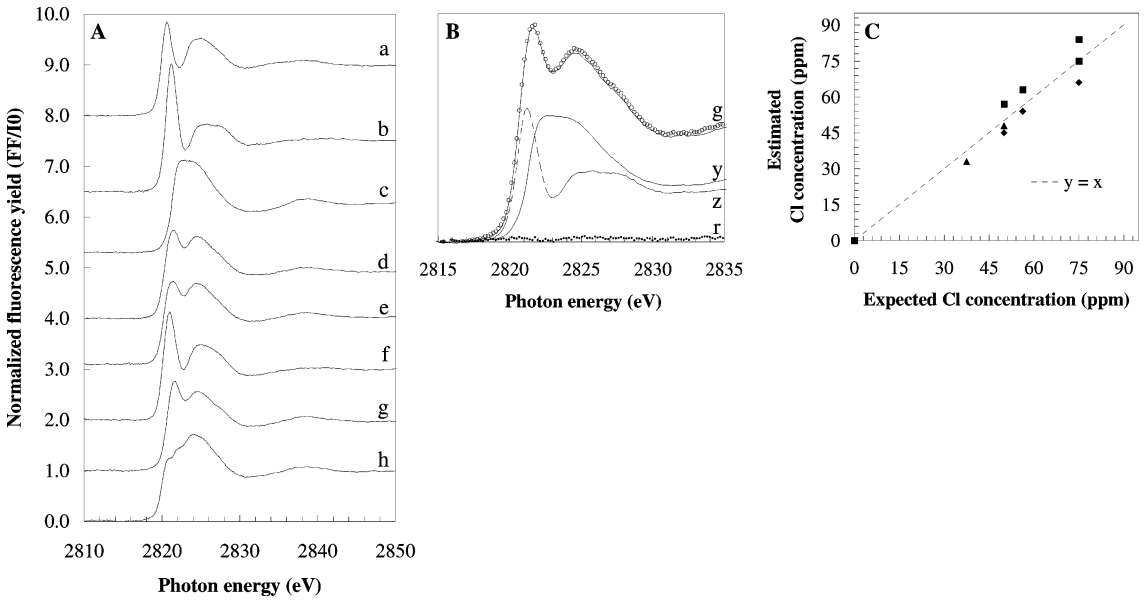

Figure 3. Speciation of Cl from Cl 1*s* XANES spectra. (A) Normalized Cl 1*s* XANES spectra of aliphatic (a, 3-chloropropionic acid), aromatic (b, chlorophenol red), and inorganic (c, NaCl) Cl standards and homogenized mixtures thereof. Spectra d−h represent the following molar Cl ratios: d, a/b/c = 0.25:0.375:0.375; e, a/b/c = 0.333:0.333:0.333; f, a/b = 0.5:0.5; g, b/c = 0.5:0.5; and h, a/c = 0.5:0.5. (B) Least-squares fit of spectrum g with spectra b and c. Spectrum g data are represented by circles and fit by the solid line; y and z show respective contributions of spectra b and c to the fit; r is the residual after the fit. (C) Estimated Cl concentrations from least-squares fits of mixed-standard spectra d−h with pure standard spectra a−c, plotted against Cl concentration expected from sample preparation. Aromatic Cl_{org} = ◆; aliphatic Cl_{org} = ▲; Cl_{inorg} = ■. Deviations of fitting results from expected Cl concentration range from 0 to 6%.

these deleterious matrix effects. To gauge the viability of this alternative, we investigated the relationship between absolute Cl fluorescence intensity and the proportion of pulverized NOM in a PAA matrix. Absolute Cl fluorescence intensity was shown to have a strong linear dependence on the fraction of NOM in the pellet (Figure 2). This relationship suggests that differences in X-ray absorption and scattering between PAA and NOM do not significantly affect fluorescence intensity; the curve would appear nonlinear if the matrixes were significantly different. This finding allows the Cl standard curve generated from PAA-based pellets to be applied to the calculation of Cl concentration in pellets prepared from pure NOM. In this way, errors due to inhomogeneous mixing of NOM and PAA are minimized.

Speciation of Cl. In addition to providing accurate Cl concentration measurements, Cl 1*s* XANES spectra illuminate the chemical forms of Cl present in a sample. The dramatic increase in X-ray absorption around 2822 eV and the surrounding spectral features correspond to electronic transitions from the Cl 1*s* shell to unoccupied molecular and atomic orbitals. Cl_{inorg} exhibits a broad absorption maximum (Figure 3A, c) markedly higher in energy than the sharper, more intense maximums characteristic of Cl_{org} compounds. These sharp peaks denote $1s \rightarrow \pi^*$ or σ^* transitions and differ in energy depending on C−Cl bond length, as becomes evident through comparison of aliphatic and aromatic Cl_{org} spectra (Figure 3A, a, b). The substantial variations in spectral features, depending on the coordination environment of Cl, allow the relative quantities of Cl_{inorg} and aliphatic and aromatic Cl_{org} in natural samples to be ascertained via least-squares fitting of sample spectra with spectra of representative model compounds, such as those in Figure 3A, a−c.

Spectra of samples prepared from homogeneous mixtures of Cl_{inorg} (as NaCl) and aliphatic and aromatic Cl_{org} (as 3-chloropropionic acid and chlorophenol red) standards show combinations of features from all three types of Cl bonding environments (Figure 3A, d−h). We have previously deconvoluted spectra of representative Cl_{org} and Cl_{inorg} compounds into their component Gaussian and Lorentzian peaks to summarize their Cl 1*s* XANES features.[26] The peak positions, widths, and relative areas vary according to the bonding state of Cl and can be used as an indicator of Cl speciation.[27] A more quantitative relationship between Cl speciation and XANES characteristics can be deduced through nonlinear least-squares fitting of spectra of the mixed standards using spectra of the pure component compounds. For instance, when this method was applied to a mixture of chlorophenol red and NaCl with Cl in equal proportions, the best fit comprised a 44% chlorophenol red spectral contribution and a 56% NaCl spectral contribution (Figure 3B). Using the pure compounds in Figure 3A, a−c, least-squares fits were obtained for all the mixtures in Figure 3A, d−h. Deviations of fitting results from the true Cl speciation in these samples ranged from 0 to 6% (Figure 3C).

High-resolution Cl 1*s* XANES spectra were collected for Cl speciation analyses with the intention of achieving higher quality spectral fits. Ultimately, however, fitting results did not prove significantly different for high- vs low-resolution spectra, as long as the Cl levels in the sample were concentrated enough to yield clean spectra (>50 ppm). For example, credible least-squares fits to the low-resolution Cl 1*s* XANES spectra acquired for Cl quantitation were used for the analysis in Table 1 (results discussed below).

Cl Measurements in NOM Samples. With proper standardization and consistent sample preparation, Cl 1*s* XANES spectra

(26) Reina, R. G.; Leri, A. C.; Myneni, S. C. B. *Environ. Sci. Technol.* **2004**, *38*, 783−789.
(27) Takahashi, Y.; Sakakibara, N.; Nomura, M. *Anal. Chem.* **2004**, *76*, 4307−4314.

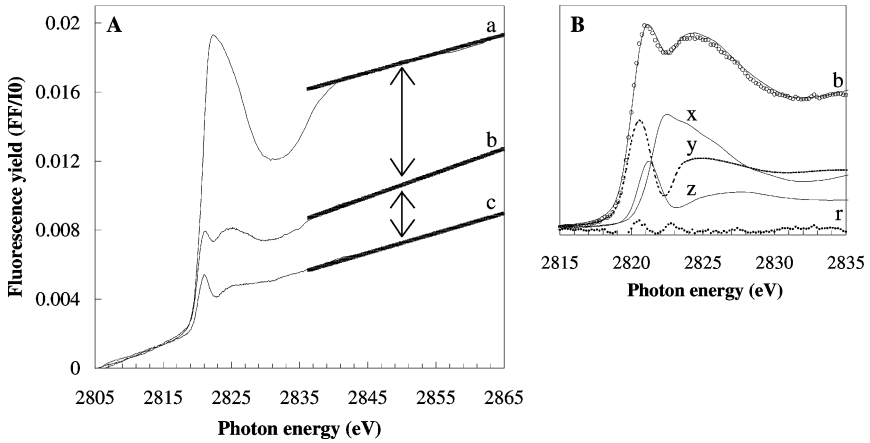

Figure 4. Determination of Cl speciation and concentration in NOM samples from Cl 1*s* XANES spectra. (A) Unnormalized Cl 1*s* XANES spectra of pulverized oak leaves at different stages of decay (a = least degraded; b = more degraded; c = most degraded). Arrows illustrate the differences in absolute Cl fluorescence intensity among the spectra. Total Cl concentrations by comparison of absolute Cl fluorescence intensity values with standard curves: a, 364; b, 141; and c, 70 ppm. (B) Least-squares fit of background-subtracted, normalized spectrum b with representative inorganic (x, glycine−HCl), aliphatic (y, chlorodecane), and aromatic (z, chlorophenol red) Cl model compounds. Spectrum b data are represented by circles and fit by the solid line; r is the residual after the fit. Estimated Cl speciation by least-squares fitting: a, 78% inorganic (284 ppm), 16% aromatic (58 ppm), 6% aliphatic (22 ppm); b, 40% inorganic (56 ppm), 20% aromatic (29 ppm), 40% aliphatic (56 ppm); c, 16% inorganic (12 ppm), 42% aromatic (29 ppm), 42% aliphatic (29 ppm).

can be used for simultaneous determination of Cl speciation and concentration in environmental samples. Unnormalized Cl 1*s* XANES spectra of oak leaf mulch at progressive stages of decay are shown in Figure 4A (a = least degraded; c = most degraded). Arrows in the postedge region of the spectra highlight the differences in absolute Cl fluorescence intensity among the spectra. Comparison of these absolute Cl fluorescence intensity values with standard curves (such as those in Figure 1B, C) yields the following total Cl concentrations: a, 364 ppm; b, 141 ppm; c, 70 ppm. The decreasing trend in Cl concentration is consistent with the leaching of soluble forms of Cl from the mulch material as part of the degradation process.

Cl speciation in natural samples can be estimated using the least-squares fitting technique described above for the standard mixtures. In the case of natural samples, errors are expected to be somewhat greater than suggested by the analysis in Figure 3C, because the model compounds selected to fit environmental spectra are only approximations of the forms of Cl that the natural samples might contain. However, high-quality fits with very small residuals convince us that Cl speciation can be reliably estimated from natural sample spectra in this manner (example, Figure 4B). The spectra used in the fits are drawn from a spectral library of several dozen model compounds with Cl in different coordination environments and oxidation states. The Cl bonding states that most consistently fit the features observed in spectra of environmental samples include aliphatic Cl_{org} (e.g., chlorodecane), aromatic Cl_{org} (e.g., chlorophenol red), H-bonded Cl_{inorg} (e.g., glycine−HCl), and fully hydrated aqueous Cl_{inorg} (e.g., HCl (aq)). Fitting the spectra in Figure 4A (after background subtraction and normalization) results in percentage estimates for Cl_{inorg}, aromatic Cl_{org}, and aliphatic Cl_{org}. Combination of these proportions with the total Cl concentrations reported above yields the concentrations of Cl_{inorg}, aromatic Cl_{org}, and aliphatic Cl_{org} in the NOM samples (Figure 4, caption). A similar analytical scheme was employed to produce the concentrations of different Cl species presented in Table 1. It should be emphasized that Cl 1*s* XANES spectra provide information on the local bonding environment of Cl only, revealing little about the comprehensive structures of Cl-containing molecules in natural samples.

Quantification of Br. XRF spectra show well-resolved Br Kα emission peaks (see Supporting Information for a representative XRF spectrum of a natural sample). Br calibration curves are generated using the area under the Br Kα peak in XRF spectra of KBr standards in a $NaNO_3$ matrix. The crystalline $NaNO_3$ matrix was selected to complement the mostly mineral character of the sediments being analyzed for Br. There is a strong linear correlation between the Br concentration in KBr standards and the area under the Br Kα emission peak (see Supporting Information). Br concentrations in environmental samples are estimated from resulting KBr standard curves.

Sediment samples would not form cohesive pellets unless mixed in some ratio with the sticky $NaNO_3$ matrix, meaning that matrix effects could not be mitigated as they were for the pure NOM pellets measured for Cl concentration. In contrast with solid NOM powder, however, finely ground sediment appeared quite miscible with the matrix, so the resulting pellets were not conspicuously heterogeneous.

Quantification of Br is more straightforward than quantification of Cl for several reasons. The XRF spectra used for Br quantification require shorter data acquisition times (~20−30×) than XANES spectra, meaning that more samples can be measured per Br standard series. In addition, whereas scattering features can complicate XANES spectra, scattering peaks in XRF spectra appear separate from elemental emission peaks, meaning that Br signals are relatively clean. Finally, since Br is a relatively high-Z element, Br X-ray data can be collected in air. By contrast, Cl 1*s* XANES spectra must be collected under He to obtain sufficient photon flux from the lower-energy X-ray beam. Inconsistent He flow into the sample chamber can affect scattering cross sections and may be partially responsible for variabilities observed in Cl calibration curves over long periods of data acquisition. Provided X-ray beam size and sample thickness/density remain consistent, Br concentration estimates are reliable and reproducible.

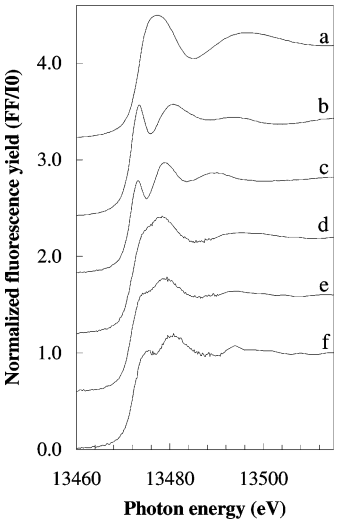

Figure 5. Normalized Br 1*s* XANES spectra of model compounds and natural samples. a, KBr (aq); b, bromophenol blue; c, 1-bromoeicosane; d, deep Bering Sea sediment; e, Chesapeake Bay estuarine sediment; and f, Cape Cod estuarine sediment.

Table 2. Br Concentrations in Sediment Samples from Different Locations

location	total Br (ppm)[a]	Br_{inorg} (ppm)[b]	Br_{org} (ppm)[b]
Bering Sea	139	79	60
Chesapeake Bay	304	91	213
Cape Cod estuary	30	12	18

[a] Total Br concentrations determined from XRF measurements. [b] Fractions of Br_{org} and Br_{inorg} estimated via least-squares fitting of sample Br 1*s* XANES spectra with those of model compounds of known coordination environment, for example, KBr (aq), bromophenol blue. Combination of these proportions with total Br concentrations gives concentrations of Br_{inorg} and Br_{org} in the sediment samples.

Speciation of Br. Total Br concentrations in environmental samples have been determined via XRF analysis for decades.[15,16] The combination of such data with the fractions of Br_{org} and Br_{inorg} as estimated from Br 1*s* XANES spectra, on the other hand, is novel. The Br K-absorption edge and its near-edge features correspond to electronic transitions from the Br-1*s* core orbitals to vacant atomic and molecular orbitals with Br-4p character. Aqueous Br_{inorg} displays a broad absorption maximum peaking at 13 477.8 eV (e.g., KBr (aq), Figure 5a). In comparison, a C−Br bond results in the appearance of discrete lower-energy peaks with maximums closer to 13 474 eV, corresponding to $1s \rightarrow \pi^*$ or σ^* molecular orbital transitions. As with Cl compounds, Br atoms connected to aromatic C display absorption maximums at higher energy than Br connected to aliphatic C (e.g., bromophenol blue vs 1-bromoeicosane, Figure 5b−c). However, at the Br K-absorption edge, the spectral resolution is too poor to quantify separate contributions of aliphatic and aromatic Br_{org} to overall Br_{org}. Br_{org} and Br_{inorg} spectra are sufficiently dissimilar for us to determine their relative concentrations in environmental samples with confidence. Br 1*s* XANES spectra of sediment samples from three different estuarine and marine locations around the globe are shown in Figure 5d−f. Least-squares fits of these spectra with those of representative Br model compounds, such as those in Figure 5a−c, quantify the contributions of Br_{org} and Br_{inorg} to the total Br signal. Uniting this information with total Br concentration values from XRF measurements yields absolute concentrations of Br_{org} and Br_{inorg} (Table 2).

CONCLUSION

Quantitative analysis of organic and inorganic halogen fractions in soil and sediment samples has been demonstrated by means of synchrotron-based X-ray absorption spectroscopy. The strong dependence of absolute fluorescence intensity in Cl 1*s* XANES spectra on Cl concentration in PAA-based NaCl standards produces reliable, linear calibration curves, from which Cl concentration in natural samples can be estimated with high precision. Comparable X-ray beam absorption and scattering by PAA-based standards and pure NOM allows for measurement of Cl concentrations in homogeneous NOM sample pellets, thus minimizing errors due to matrix effects. The fractions of Cl_{inorg}, aliphatic Cl_{org}, and aromatic Cl_{org} contributing to the total Cl 1*s* XANES signal are computed through spectral fitting with errors on the order of ~6%. Cl 1*s* XANES spectroscopy thus permits total Cl_{inorg}, aliphatic Cl_{org}, and aromatic Cl_{org} concentrations to be determined simultaneously in environmental samples. The concentrations of Br_{org} and Br_{inorg} in sediment samples were also measured using a combination of synchrotron-based XRF and Br 1*s* XANES spectroscopy. This method provides a rigorous new approach to the determination of absolute organohalogen concentrations in complex natural samples in situ. An analogous procedure can be applied to other elements, as well; we are in the process of quantifying different forms of S in environmental samples on the basis of S 1*s* XANES spectroscopy.

ACKNOWLEDGMENT

Financial support for this work was provided by the U.S. Department of Energy, Office of Basic Energy Sciences (DOE-BES) Chemical and Geosciences Programs, the National Science Foundation (NSF) Chemical Sciences Program, and NSF Graduate Research Fellowships (A.C.L. and M.B.H.). Use of the National Synchrotron Light Source, Brookhaven National Laboratory, was supported by the DOE-BES under Contract No. DE-AC02-98CH10886. Use of the Stanford Synchrotron Radiation Laboratory, a national user facility operated by Stanford University, was also supported by the DOE-BES. We thank Wolfgang Caliebe, Syed Khalid, and Christie Nelson of the NSLS and the SSRL staff scientists for beamline support. We thank Bess Ward and Daniel Sigman of Princeton University and Christopher Reddy of Woods Hole Oceanographic Institute for providing sediment samples. Portions of this work were performed at Beamlines X19A and X26A at the NSLS. Beamline X19A is a facility beamline operated and managed by the NSLS. Beamline X26A is supported by the DOE−Geosciences (DE-FG02-92ER14244 to the University of Chicago−CARS) and DOE−Office of Biological and Environmental Research, Environmental Remediation Sciences Division (DE-FC09-96-SR18546 to the University of Georgia).

SUPPORTING INFORMATION AVAILABLE

Supporting Information as noted in text. This material is available free of charge via the Internet at http://pubs.acs.org.

Received for review March 15, 2006. Accepted June 21, 2006.

AC060476M